RESEARCH PAPER
Contrib. Sci. & Tech Eng, 2026, 3(1)
Homepage: https://cste.journals.umz.ac.ir/
DOI: 10.22080/cste.2025.29067.1035

A High-Gain, Low CRR, Narrow beam width Enhanced Vivaldi Antenna for Through-the- Wall Imaging Radar

Armin Mohammadjany [1], Hossein Miar-Naimi [2]*

[1] *Ph.D. Candidate, Department of Electrical and Electronic Engineering, Babol Noshirvani University of Technology, Babol, Iran.*

[2] *Professor, Department of Electrical and Electronic Engineering, Babol Noshirvani University of Technology, Babol, Iran.*

Article Info
Received 22 April 2025
Accepted 08 July 2025
Available online 08 January 2026

Keywords:
TWIR;
Vivaldi Antennas;
Tapered Slot Antennas;
Microwave Imaging.

Abstract:
This study presents an optimized ultra-wideband (UWB) Vivaldi antenna engineered for high gain, narrow beamwidth, and superior impedance matching, designed explicitly for Through-the-Wall Imaging Radar (TWIR) systems. Fabricated on a cost-effective 0.8-mm-thick FR-4 substrate with dimensions of 148 mm × 85 mm, the antenna incorporates ten open-ended rectangular slits on each arm of the exponentially tapered slot and nine metallic strips at the slot's end. Through extensive parametric optimization and precise positioning, this configuration uniquely enhances gain by 51% at lower frequencies and 35% at 4 GHz compared to conventional designs, peaking at 12.59 dBi. Operating across 1.9 to 4.5 GHz, it delivers gains exceeding 7 dBi from 2.3 to 4.5 GHz and a narrow beamwidth down to 29.3° at 4 GHz. Validated by CST Microwave Studio simulations and measurements, this antenna outperforms existing TWIR-focused Vivaldi designs in penetration and resolution, making it an exceptional candidate for advanced radar imaging applications.

***Corresponding Author:** h_miare@nit.ac.ir

Supplementary information: Supplementary information for this article is available at https://cste.journals.umz.ac.ir/

Please cite this paper as: Mohammadjany, A., & Miar-Naimi, H. (2026). A High-Gain, Low CRR, Narrow beam width Enhanced Vivaldi Antenna for Through-the- Wall Imaging Radar. Contributions of Science and Technology for Engineering, 3(1), 1-9. doi:10.22080/cste.2025.29067.1035.

1. Introduction

The rapid advancement of satellite, wireless communication, and radar technologies has given rise to the emergence of Ultra-Wide Band (UWB) electronic systems. A radio communication system is defined as UWB if its signal spectrum covers a bandwidth exceeding 20% of the center frequency or surpassing 500MHz [1]. UWB technology demands antennas with a broad bandwidth and the ability to minimize distortion in both transmitted and received signals. Radar technology possesses the capability to accurately identify can accurately determine an object's position, distance, and velocity. For example, through the Wall Imaging Radar (TWIR) in military-security operations, the Ground Penetrating Radar (GPR) in civil engineering, and a cancer cell detection system in medical facilities, these issues can be addressed [2-5]. One of the essential components of radar is the antenna. The antenna's specification will determine the radar's performance when designing a radar. Tapered Slot Antennas (TSA) are among the most suitable choices for UWB technology applications. These antennas provide wide bandwidth, high gain, and directive propagation at these frequencies, with symmetric radiation patterns in both co- and cross-polarization [6, 7]. TSAs are practical, portable, and compact. Additionally, their relatively simple geometry enhances their advantages. The Vivaldi antenna stands out as the most widely utilized TSA in UWB technology applications. It was initially introduced by Gibson in 1979 [6] and later modified into a tapered-slot antenna by Lewis et al. [8]. An exponentially tapered slot line is characteristic of the Vivaldi antenna. Thanks to the use of printed circuit technology for fabrication, these antennas are cost-effective and relatively unaffected by dimensional tolerances. Additionally, Vivaldi arrays are compact and lightweight, making them an ideal choice for compact arrays [9]. It's important to note that adjusting the design parameters can significantly enhance the beam width and directivity of a Vivaldi antenna.

In this article, we aim to develop an effective antenna for TWIR applications. Figure 1 depicts the block diagram of a monostatic TWIR system. Given the suitability of Vivaldi antennas for UWB applications, their design must address specific challenges in Through-the-Wall Imaging Radar (TWIR). Signal attenuation through materials such as concrete increases significantly above 8 GHz, as shown in Figure 2 [10], favoring lower frequencies (e.g., 2–8 GHz) for penetration [11]. Yet, in synthetic aperture radar (SAR), cross-range resolution (CRR) improves with smaller apertures (D), limited to D/2 [12], though reducing size typically increases operating frequency, reducing penetration. The key challenge is crafting a compact Vivaldi

*ISSN **3060-6578***

antenna that retains low-frequency performance for deep penetration while enhancing CRR. This study tackles this by optimizing a UWB Vivaldi design with slits and metallic strips, achieving high gain and directivity within 1.9–4.5 GHz with a footprint of 148 mm × 85 mm. This optimized antenna features an extensive operating bandwidth from 1.9 GHz to 4.5 GHz and a gain exceeding 7 dBi across 2.3 GHz to 4.5 GHz. It shows a maximum gain of 12.59 dBi at 4 GHz and 10.27 dBi at the center of the S-band at 3 GHz. The rest of the paper is as follows: In Section 2, we will outline the proposed design for the improved Vivaldi antenna. Section 3 consolidates the simulation results and validates those using experimental data. Finally, Section 4 expresses conclusions.

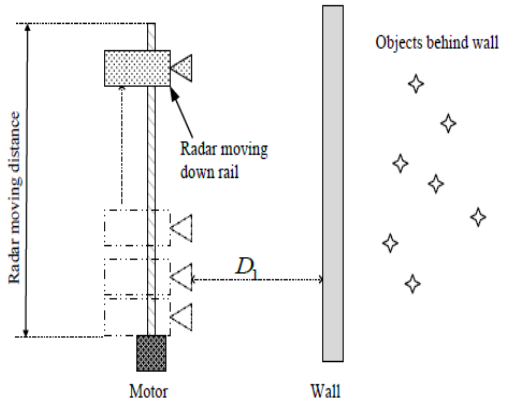

Figure 1. TWIR SAR geometry by Dehmollaian et al. [13]

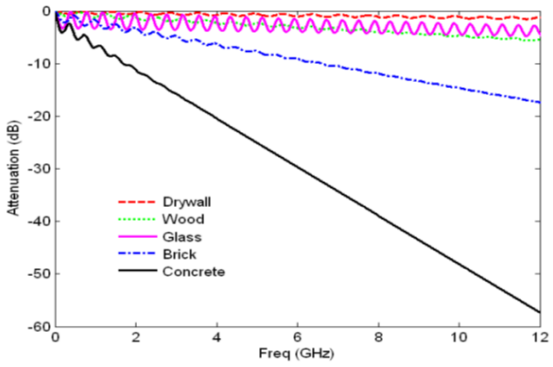

Figure 2. One-way through wall transmission through various building materials, with a thickness of 6 inch [11].

2. Design of the Antenna

2.1. Antenna Structure and Geometry

The geometry of the Vivaldi antenna intended for TWIR applications is illustrated in Figure 3. This antenna consists of three distinct layers, in which the upper layer includes a rectangular slot that transitions into an exponentially tapered slot at one extremity and a circular slot at the other [6]. The slot is crafted in an exponentially tapered profile to efficiently emit traveling waves and ensure robust impedance matching over a broad frequency range [14]. The curve of this slot, labelled as C1, follows the exponential equation $y = \pm We^{\alpha x}$, where W=0.25 mm represents half the slot width at the origin, and α=0.051 is the opening rate determining the taper's slope. This configuration, optimized through simulations, enhances radiation efficiency and supports the antenna's broadband performance.

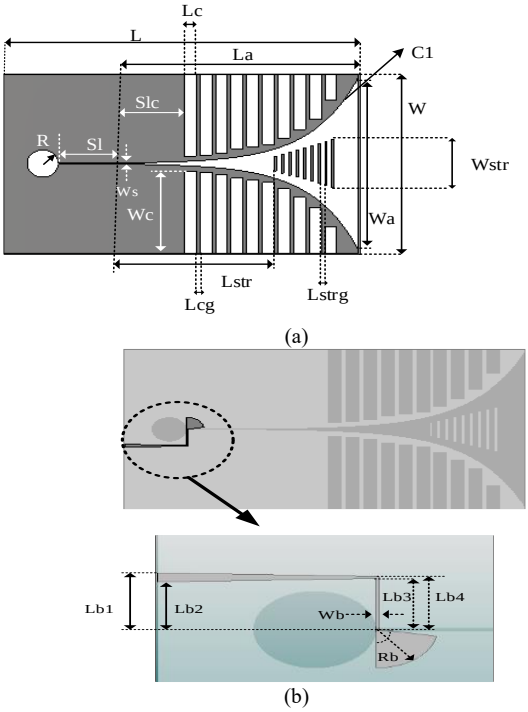

Figure 3. Geometry of the proposed antenna. (a) Top view. (b) Bottom view

The bottom layer serves as the antenna's feed. For optimal performance within the TSA class, the Vivaldi antenna performs best when integrated with a slot-line feeding mechanism. Therefore, a transition is necessary to effectively transfer signals between the transmitter or receiver circuitry and the Vivaldi slot line. This transition should have minimal signal loss across a wide frequency range, ensuring the operating bandwidth is not restricted. In addition, it should be compact and easy to manufacture. In this transition, electromagnetic fields enable efficient coupling of signals to the slot line. This paper uses a stripline-to-slot transition with a radial stub to achieve maximum bandwidth, as shown in Figure 3-b. A cross junction is created at the intersection of the microstrip and the slot line, forming a right angle. At the cross junction, the microstrip line functions as a short circuit because the radial stub is approximately a quarter wavelength long [15], while the end of the circuit remains open. The emitted energy produces an end-fire radiation pattern as energy moves from the microstrip line to the slot line and emanates through the exponentially tapered slot. Ten open-ended rectangular slits, each 5 mm wide with a 1.5 mm spacing, are embedded along each arm of the exponentially tapered slot. These slits, with dimensions, number, and placement optimized via extensive CST Microwave Studio simulations, adjust surface current distribution to improve impedance matching, extend low-frequency bandwidth, and concentrate the electric field in the tapered slot for enhanced radiation efficiency. Nine metallic strips at the slot's end, similarly optimized through CST simulations, serve as parasitic directors to focus radiated energy, narrow the beamwidth, and improve cross-range resolution (CRR) for high-resolution TWIR imaging [16]. This configuration aligns with the antenna's compact 148 mm × 85 mm footprint, tailored for TWIR applications. Detailed geometric characteristics are provided in Tables 1 and 2.

The chosen substrate for this design is a low-cost, 0.8-mm-thick FR-4 material with a dielectric constant of 4.4 and a loss tangent of 0.025. While FR-4 exhibits higher losses than premium substrates, its affordability drove its selection, with the inclusion of ten slits and nine strips along the tapered slot compensating for these limitations by refining the field distribution, as elaborated in Section 3.

Table 1. Key Design Parameters Of The Proposed Design

Parameter	Dimension(mm)	Note
L	148	Substrate length
W	85	Substrate width
La	100	Curve length
Wa	82	Curve width
Lc	5	slit width
Lcg	1.5	Gape between two slit's
Slc	27.5	Distance to first slit from origin
Lstr	65	Distance to the first metallic strip from the origin
Lstrg	2	Gape between two strips
Sl	25	Slot length
Ws	0.5	Slot width
R	6.46	Cavity radius
Wb	0.323	Second stub feed slot width
Rb	6.46	Radius of radial stub
Lb1	9.518	Distance from the outer edge of the first stub to the origin axes.
Lb2	8	Distance from the inner edge of the first stub to the origin axes
Lb3	8.5975	Distance from the outer edge of the second stub to the origin axes.
Lb4	8.9205	Distance from the inner edge of the second stub to the origin axes

Table 2. Geometric Characteristics of Slits and Metallic Strips

Parameter	Wc0	Wc1	Wc2	Wc3	Wc4
Dimension (mm)	39	38.5	37.5	35.5	34.5
Parameter	Wc5	Wc6	Wc7	Wc8	Wc9
Dimension (mm)	33.5	30.5	26.5	21.5	12.5
Parameter	Wstr0	Wstr1	Wstr2	Wstr3	Wstr4
Dimension (mm)	7	9	11	13	15
Parameter	Wstr5	Wstr6	Wstr7	Wstr8	
Dimension (mm)	17	19	21	23	

2.2. Design Process

To clarify the proposed antenna's design guidelines, the evolutionary process is depicted in Figure 4, which illustrates the progression from Antenna 1 to Antenna 3. Antenna 1 shows the basic design of the Vivaldi antenna; it features an exponentially tapered conical slot paired with a 50 Ω feed line. Antenna 2 enhances this configuration by incorporating two groups of open-ended rectangular slits on each arm of the exponentially shaped slot. Lastly, Antenna 3, our proposed design, is developed by attaching metal strips to the end of the tapered slot in Antenna 2.

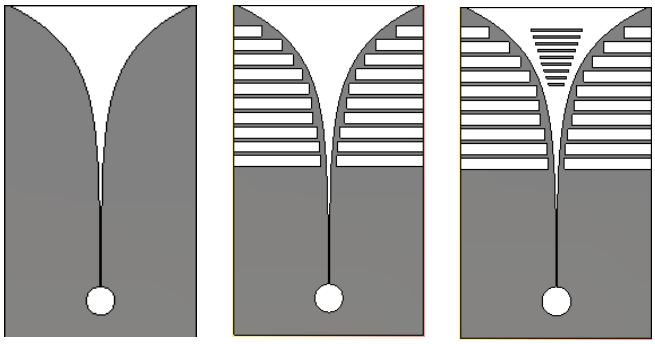

Figure 4. Geometry of different antennas. (a) Antenna 1. (b) Antenna 2. (c) Antenna 3

The graph in Figure 5-a shows the simulated reflection coefficients of Antennas 1–3. The reflection coefficient for Antenna 1 is greater than -10 dB below 3.2 GHz, making it unsuitable for the TWIR application within the desired frequency band. Nevertheless, Antenna 2, enhanced by the inclusion of rectangular slits, provides outstanding -10 dB in the low-frequency range, which satisfies the needs of real-world applications. Likewise, Antenna 3 exhibits superb impedance matching, maintaining a reflection coefficient below -10dB across the 1.9 to 4.5 GHz frequency band. It's worth highlighting that the rectangular slits are crucial for ensuring impedance matching in the low-frequency range. The simulated gain figures for Antennas 1 through 3 are presented in Figure 5-b. As shown, adding slots on both sides of the conical groove has significantly increased the gain of antenna 2 across the entire band compared to antenna 1. Specifically, the gain noticeably increases at 2, 3, and 4 GHz from 4.33 to 6.54 dBi, 6.5 to 8 dBi, and 8 to 9.3 dBi, respectively. The gain shows a significant increase in the 2.4 to 3.4 GHz range for the ultimate antenna featuring the metal strip design. Owing to the metallic strips, the electric field exhibits a significantly greater concentration near the tapered slot in Antenna 3 than in Antenna 2. This rise underscores the intriguing role of metallic strips at the ends of the tapered slot in enhancing gain, in addition to the open-end rectangular slits.

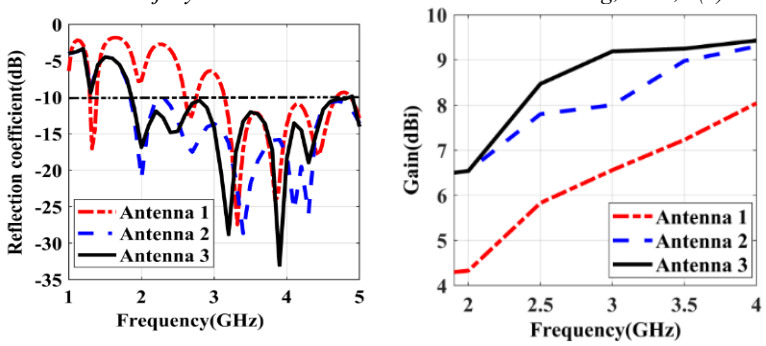

(a) (b)

Figure 5. Simulated (a) reflection coefficients and (b) gains of different antennas

For a clearer view of the enhanced pattern symmetry, the radiation patterns at 2, 3, and 4 GHz are also provided, as shown in Figure 6. Antenna 1's main lobe beam squint is 0°, 7°, and 3° at 2, 3, and 4 GHz, respectively. For antennas 2 and 3, the main lobe beam squints at the mentioned frequencies are (0°, 0°, 0°) and (0°, 1°, 2°), respectively. The addition of open-end rectangular slits to antenna 2 has significantly improved the main lobe beam squint and the asymmetrical radiation pattern in the E-plane compared to those of antenna 1. Additionally, metallic strips in the final structure are valuable for increasing gain, albeit at the cost of a slight deviation of the main lobe. Overall, the proposed antenna achieves remarkably symmetric radiation patterns.

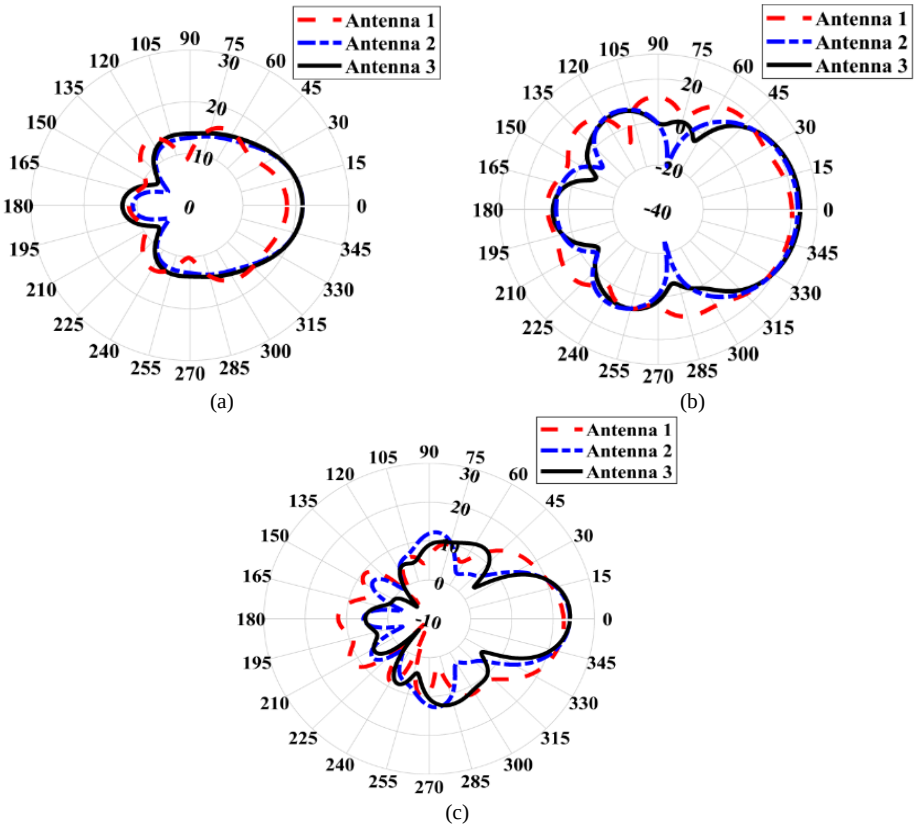

(a) (b) (c)

Figure 6. Antenna radiation patterns displayed at frequencies of (a) 2 GHz, (b) 3 GHz, and (c) 4 GHz

For a clearer view of the enhanced pattern symmetry, the radiation patterns at 2, 3, and 4 GHz are also provided, as shown in Figure 6. Antenna 1's main lobe beam squint is 0°, 7°, and 3° at 2, 3, and 4 GHz, respectively. For antennas 2 and 3, the main lobe beam squints at the mentioned frequencies are (0°, 0°, 0°) and (0°, 1°, 2°), respectively. The addition of open-end rectangular slits to antenna 2 has significantly improved the main lobe beam squint and the asymmetrical radiation pattern in the E-plane compared to those of antenna 1. Additionally, metallic strips in the final structure are valuable for increasing gain, albeit at the cost of a slight deviation of the main lobe. Overall, the proposed antenna achieves remarkably symmetric radiation patterns.

2.3. Manufacturing Tolerance Robustness

To evaluate the robustness of the proposed Vivaldi antenna against manufacturing tolerances, we assessed the practical performance of the fabricated prototype, constructed on an FR-4 substrate using standard PCB processes with typical tolerances of ±0.1 mm. Despite these inherent manufacturing inaccuracies, the measured performance closely aligns with CST Microwave Studio simulations, as

evidenced by the reflection coefficient below −10 dB across 1.9–4.5 GHz (Figure 5-a), peak gain of 12.59 dBi at 4 GHz (Figure 7), 3-dB beamwidth of 29.1° (Table 3), and cross-range resolution (CRR) of 42.5 mm. This consistency between simulated and measured results indicates that the antenna's performance remains stable under real-world fabrication variations. The robust field distribution, driven by the optimized configuration of ten rectangular slits and nine metallic strips (Section 2.1), mitigates the impact of minor dimensional inaccuracies, ensuring reliable operation for Through-the-Wall Imaging Radar (TWIR) applications. While a comprehensive sensitivity analysis of slit and strip dimensions is planned for future work to quantify further robustness, the successful fabrication and testing of the prototype, supported by measurements in Section 3, demonstrate the design's practical resilience to manufacturing tolerances.

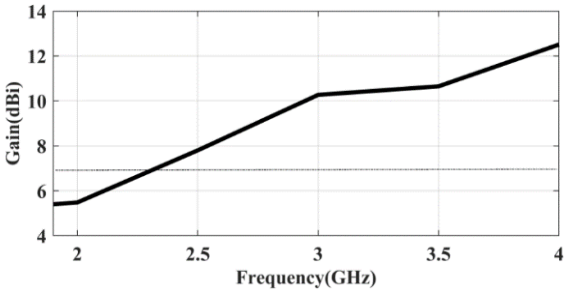

Figure 7. Measured gain of the proposed antenna

Table 3. Comparing Earlier Vivaldi Antenna Studies with the Proposed Antenna Design

Ref	Substrate	Best CRR (mm)	Freq. (GHz): Max gain(dBi): MinΘ_{3dB}	Operating band (GHz)	Antenna size(mm)	Year
Kuriakose et al. [16]	FR4	35	4.5:8.2: 52°	1.9-12	70×128	2020
Cam et al. [17]	FR4	45.5	2.5:7.66:N.S	1-4	91×108	2017
Kumar et al. [18]	FR4	70	2.6:10: 31°	0.8-4	140×200	2016
Tahar et al. [19]	FR4	50	3:8.39:54.2°	1.17-4.75	100×200	2018
Ahmed et al. [20]	RO 5880	30.37	10:11.5: 59.8°	3.1-10.6	60.75×66	2023
Zhang et al. [21]	RO 4350B	40.5	6.3:9.7: 53°	4-8	81×110	2020
Murphy et al. [22]	RO4350	N.S	4.2: 18 (3×3 array)/9 (1×3 subarray): 21° (azimuth, 3×3 array)	3.1–5.3	N.S (3×3 array)	2018
This work	FR4	42.5	4:12.59:29.3°	1.9-4.5	85×148	

3. Measurement

The proposed Vivaldi antenna prototype, based on the Antenna 3 design with slits and metallic strips, was constructed and tested. Figure 8 shows a photo of the prototype, and Figures 9 and 10 display the measured reflection coefficient and Voltage Standing Wave Ratio (VSWR) compared to the simulated values. As depicted in Figure 9, the antenna demonstrates excellent impedance matching across the 1.9 to 4.5 GHz range. The measured reflection coefficient is below -10 dB across this frequency range, and the VSWR is below 2, confirming that the antenna is well-matched (Figure 10).

(a)

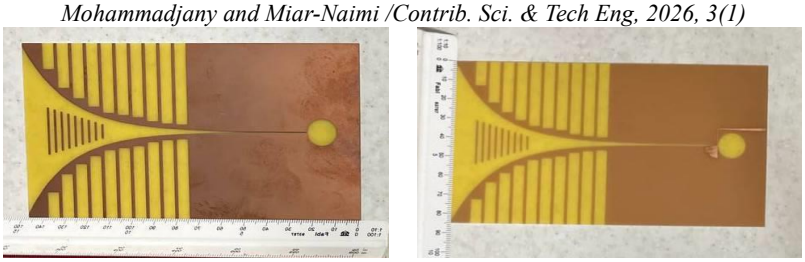

(b) (c)

Figure 8. Photograph of the fabricated antenna. (a) Overview of both sides of the fabricated antenna. (b) Front view. (c) Back view

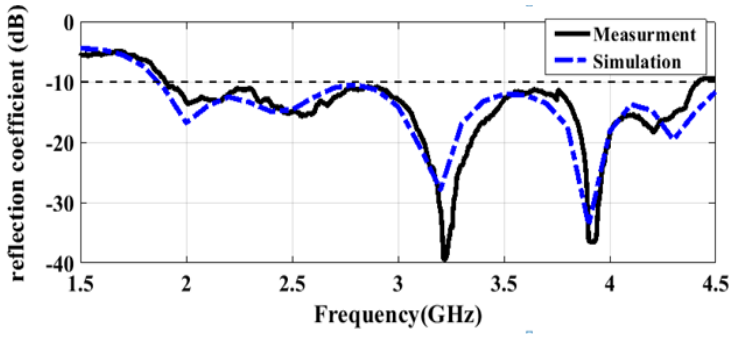

Figure 9. Measured and simulated reflection coefficient of the antenna

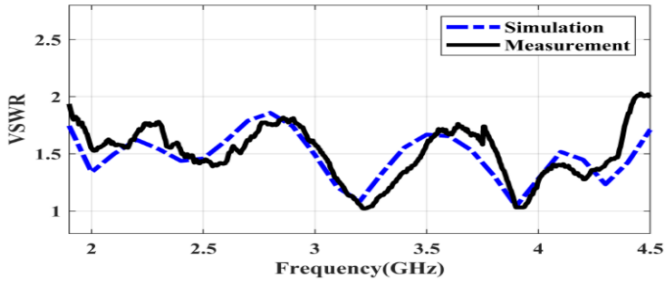

Figure 10. Measured and simulated VSWR of the antenna

Figures 11-a to 11-e illustrate the measured and simulated radiation patterns of the proposed Vivaldi antenna at 2, 2.5, 3, 3.5, and 4 GHz, respectively. These results, obtained from the fabricated Antenna 3, show that the simulated outcomes align closely with the measured data, with discrepancies typically below 1 dB, reflecting strong consistency due to the optimized design and precise simulation. The main lobe has a narrow 3dB beam width of 57°, 55.2°, 55.2°, 38.3°, and 29.3° at 2, 2.5, 3, 3.5, and 4 GHz, respectively. The high gain and low VSWR confirm that the slits and strips effectively mitigate the higher losses of FR-4, aligning with the design goals. Figure 7 presents the measured gain of the designed antenna. The gain ranges from 5.40 dBi at 1.9 GHz to 12.59 dBi at 4 GHz within the 1.9 to 4.5 GHz operating band, exceeding 7 dBi from 2.5 to 4.5 GHz, with measured values of 5.5 dBi at 2 GHz, 7.8 dBi at 2.5 GHz, 10.27 dBi at 3 GHz, 10.5 dBi at 3.5 GHz, and a peak of 12.59 dBi at 4 GHz.

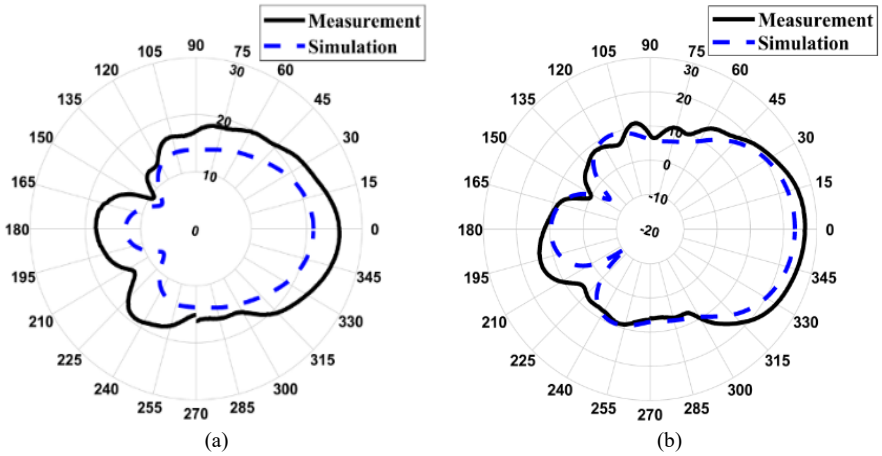

(a) (b)

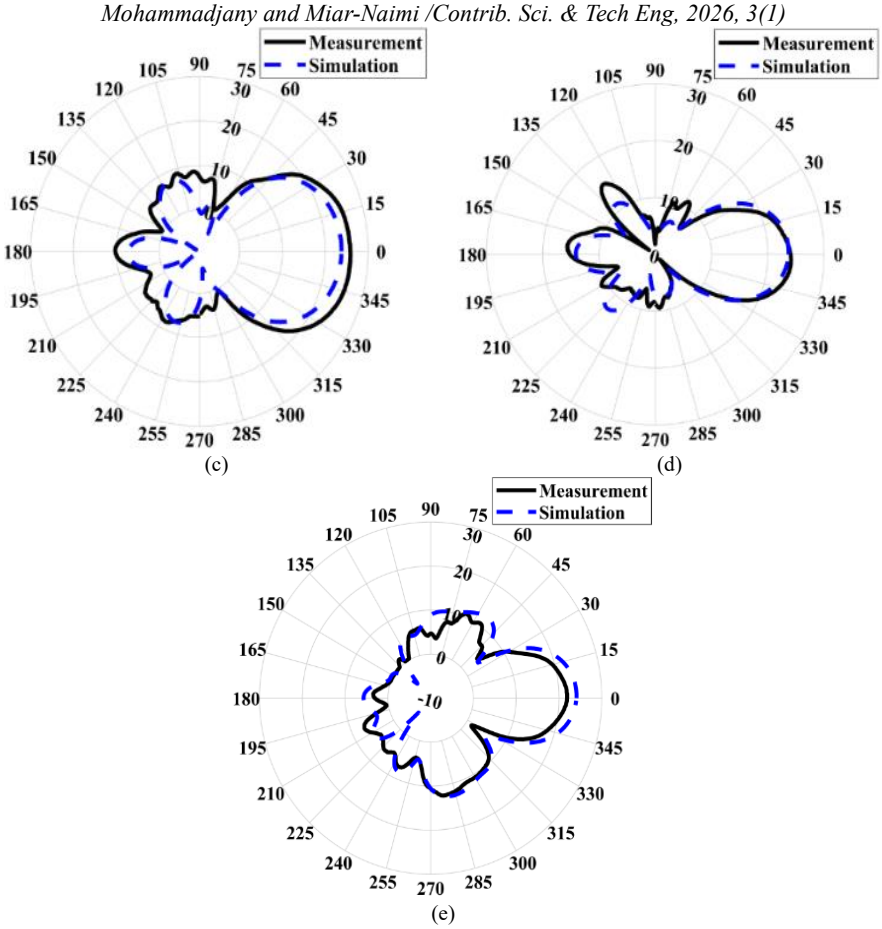

Figure 11. Measured and simulated radiation pattern of the proposed antenna at (a) 2, (b) 2.5,(c)3,(d)3.5, and (e) 4 GHz

Table 3 compares the antenna parameters of the proposed Vivaldi antenna with those from other relevant studies, including References [16-22]. The proposed antenna, fabricated on a cost-effective FR-4 substrate with a compact size of 148 × 85 mm, achieves a peak gain of 12.59 dBi at 4 GHz, a 3-dB beamwidth of 29.3° at 4 GHz, and a cross-range resolution (CRR) of 42.5 mm, while covering a low-frequency range of 1.9–4.5 GHz—critical for wall penetration in Through the-Wall Imaging Radar (TWIR). Compared to Kuriakose et al. [16], which offers a gain of 8.2 dBi and a wider beamwidth of 52° at 4.5 GHz, the proposed design provides significantly higher gain and a narrower beamwidth. Cam et al. [17] achieve a lower gain of 7.66 dBi at 2.5 GHz and a CRR of 45.5 mm, while Kumar et al. [18] report a gain of 10 dBi at 2.6 GHz but with a larger size (140 × 200 mm) and a CRR of 70 mm, both less competitive than the proposed antenna. Tahar et al. [19] have a comparable CRR (50 mm) but a lower gain (8.39 dBi) and a wider beamwidth (54.2°). Reference [20], using a premium RO5880 substrate, achieves a high gain of 11.5 dBi at 10 GHz and a CRR of 30.37 mm but operates at higher frequencies (3.1–10.6 GHz), limiting its low-frequency penetration for TWIR. Ahmed et al. [21], which employs a gain-enhanced Vivaldi antenna on an RO4350B substrate for handheld TWIR, reports a gain of 9.7 dBi at 6.3 GHz, a beamwidth of 53°, and a CRR of 40.5 mm in the 4–8 GHz range. Murphy et al. [22], which presents a 3×3 Vivaldi antenna array for 3D radar imaging, achieves a gain of 18 dBi at 4.2 GHz for the full array and 9 dBi for a 1×3 subarray, with a beamwidth of 21° in the azimuthal plane for the whole array, operating in the 3.1–5.3 GHz range. Compared to Murphy et al. [22], the proposed single-element antenna offers a higher gain than the 1×3 subarray (12.59 dBi vs. 9 dBi). It operates at a lower frequency (1.9 GHz vs. 3.1 GHz), making it more suitable for compact, low-frequency TWIR applications, despite a slightly higher CRR (42.5 mm vs. 40.5 mm in Ahmed et al. [21] and unspecified in Murphy et al. [22]). The proposed design strikes a critical balance: its compact size enhances CRR without compromising low-frequency penetration. At the same time, its high gain and narrow beamwidth ensure superior directivity and imaging quality, making it exceptionally suited for TWIR applications.

As detailed in Table 3 and the preceding comparison, the proposed Vivaldi antenna excels in key metrics for Through-the-Wall Imaging Radar (TWIR), surpassing prior works [16-22]. The design's qualitative advantages arise from its innovative features, which underpin its exceptional performance. The ten rectangular slits and nine metallic strips, optimized using CST Microwave Studio, enhance electric-field concentration and suppress sidelobes, enabling precise imaging with superior cross-range resolution, unlike the less-focused patterns reported by Kuriakose et al. [16] and Tahar et al. [19]. This configuration enables deep penetration at 1.9 GHz, which is critical for traversing dielectric barriers such as concrete in military or rescue scenarios, where Ahmed et al.'s [20] higher-frequency operation falls short. The compact footprint, achieved without sacrificing performance, ensures portability for handheld TWIR systems, in contrast to Kumar et al.'s [18] bulkier structure. Using a cost-effective FR-4 substrate, compensated by an optimized field

distribution, reduces costs compared to premium substrates, as reported by Ahmed et al. [20] and Zhang et al. [21], thereby broadening accessibility for practical TWIR deployments. Unlike Murphy et al.'s [22] complex 3×3 array, the single-element design simplifies fabrication and integration, offering a practical balance between performance and cost. These tailored features—optimized field control, low-frequency penetration, portability, and affordability—make the proposed antenna uniquely effective for TWIR's demanding requirements.

4. Conclusion

This article introduces the design of a high-gain, narrow-beam UWB Vivaldi antenna, with dimensions of 148 mm × 85 mm, realized on a cost-effective FR-4 substrate. This design guarantees effective impedance matching, achieving a reflection coefficient below −10 dB, while providing consistent and well-balanced radiation across the 1.9 to 4.5 GHz frequency band. Additionally, it attains a gain exceeding 7 dBi across the frequency band from 2.3 GHz to 4.5 GHz, reaching a peak gain of 12.59 dBi at 4 GHz. High gain and narrow beam, particularly within the lower frequency range of 2 to 8 GHz, significantly increase the possibility of penetrating different material walls. The appropriate dimension of the designed antenna makes a suitable CRR achievable. Moreover, its planar configuration enables the proposed antenna to be manufactured economically. This balanced design optimizes size, low-frequency penetration, and gain, enhancing TWIR performance. Moreover, an ensemble of Vivaldi antenna elements can be precisely optimized to augment gain and diminish overall dimensions, tailored for extended-range radar systems. The proposed antenna possesses these features, making it highly suitable for TWIR applications.

5. References

[1] Federal Communication Commission. (2002). First Order and Report. Revision of Part 15 of the Commission's Rules Regarding UWB Transmissions Systems, FCC 02-48, Federal Communication Commission, Washington, United States.

[2] Hoang, T. V., Kumar, R., Fromenteze, T., Garcia-Fernandez, M., Alvarez-Narciandi, G., Fusco, V., & Yurduseven, O. (2022). Frequency Selective Computational Through Wall Imaging Using a Dynamically Reconfigurable Metasurface Aperture. IEEE Open Journal of Antennas and Propagation, 3, 353–362. doi:10.1109/OJAP.2022.3161128.

[3] Fedeli, A., Pastorino, M., Ponti, C., Randazzo, A., & Schettini, G. (2020). Through-the-wall microwave imaging: Forward and inverse scattering modeling. Sensors (Switzerland), 20(10), 2865. doi:10.3390/s20102865.

[4] Mu, K., Luan, T. H., Zhu, L., Cai, L. X., & Gao, L. (2020). A Survey of Handy See-Through Wall Technology. IEEE Access, 8, 82951–82971. doi:10.1109/ACCESS.2020.2991201.

[5] 5 Angel, J. J., & Jones Mary, T. A. (2014). Design of Vivaldi antenna for brain cancer detection. 2014 International Conference on Electronics and Communication Systems (ICECS), 1–4. doi:10.1109/ecs.2014.6892759.

[6] Gibson, P. J. (1979). The Vivaldi Aerial. 1979 9th European Microwave Conference. doi:10.1109/euma.1979.332681.

[7] Deng, C., & Xie, Y. J. (2009). Design of resistive loading Vivaldi antenna. IEEE Antennas and Wireless Propagation Letters, 8, 240–243. doi:10.1109/LAWP.2009.2013730.

[8] Lewis, L., Fassett, M., & Hunt, J. (1974). A broadband stripline array element. 1974 Antennas and Propagation Society International Symposium. doi:10.1109/aps.1974.1147206.

[9] Erdoğan, Y. (2009). Parametric study and design of vivaldi antennas and arrays . Master Thesis, Middle East Technical University, Ankara, Turkey.

[10] Wang, Y. (2012). UWB Pulse Radar for Human Imaging and Doppler Detection Applications. PhD Thesis, University of Tennessee, Knoxville, United States.

[11] Amin, M. G. (Ed.). (2017). Through-the-wall radar imaging. CRC Press, Boca Raton, United States.

[12] Edwards, M. C. (2009). Design of a continuous-wave synthetic aperture radar system with analog dechirp. Brigham Young University, Provo, United States.

[13] Dehmollaian, M., Thiel, M., & Sarabandi, K. (2009). Through-the-wall imaging using differential SAR. IEEE Transactions on Geoscience and Remote Sensing, 47(5), 1289–1296. doi:10.1109/TGRS.2008.2010052.

[14] Shi, X., Cao, Y., Hu, Y., Luo, X., Yang, H., & Ye, L. H. (2021). A High-Gain Antipodal Vivaldi Antenna with Director and Metamaterial at 1-28 GHz. IEEE Antennas and Wireless Propagation Letters, 20(12), 2432–2436. doi:10.1109/LAWP.2021.3114061.

[15] Kumar, B., Vardhan, K. A., & Sharma, P. (2016, December). Design of slotted Vivaldi antenna for through wall imaging system. 2016 11th International Conference on Industrial and Information Systems (ICIIS), 3 to 4 December, 2016, Roorkee, India.

[16] Kuriakose, A., George, T. A., & S, A. (2020). Improved High Gain Vivaldi Antenna Design for Through-wall Radar Applications. 2020 International Symposium on Antennas & Propagation (APSYM), 58–61. doi:10.1109/apsym50265.2020.9350711.

[17] Cam, V. P., Van Tran, S., & Nguyen, D. B. (2018). An array of antipodal Vivaldi antenna with genetic optimization. 2018 International Conference on Advanced Technologies for Communications (ATC), 142–145. doi:10.1109/atc.2018.8587486.

[18] Kumar, B., Vardhan, K. A., & Sharma, P. (2016). Design of slotted Vivaldi antenna for through wall imaging system. 2016 11th International Conference on Industrial and Information Systems (ICIIS), 704–709. doi:10.1109/iciinfs.2016.8263029.

[19] Tahar, Z., Derobert, X., & Benslama, M. (2018). An Ultra-Wideband Modified Vivaldi Antenna Applied to through the Ground and Wall Imaging. Progress in Electromagnetics Research C, 86, 111–122. doi:10.2528/pierc18051502.

[20] Ahmed, S., Joret, A., Katiran, N., Liew Abdullah, M. F., Zakaria, Z., & Sulong, M. S. (2023). Ultra-wide band

antipodal Vivaldi antenna design using target detection algorithm for detection application. Bulletin of Electrical Engineering and Informatics, 12(4), 2165–2172. doi:10.11591/eei.v12i4.5081.

[21] Zhang, J., Lan, H., Liu, M., & Yang, Y. (2020). A Handheld Nano Through-Wall Radar Locating with the Gain-Enhanced Vivaldi Antenna. IEEE Sensors Journal, 20(8), 4420–4429. doi:10.1109/JSEN.2019.2963234.

[22] Murphy, C., Popovici, E., & Greenhalgh, P. (2018). Antenna Design for a 3D Image Radar System. 2018 29th Irish Signals and Systems Conference (ISSC), 1–6. doi:10.1109/issc.2018.8585382.